A Novel Pathway of Atmospheric Sulfate Formation Through Carbonate Radical

Yangyang Liu[1,2], Yue Deng[1,2], Jiarong Liu[3], Xiaozhong Fang[1], Tao Wang[1], Kejian Li[1], Kedong Gong[1], Aziz U. Bacha[1], Iqra Nabi[1], Xiuhui Zhang[3], Christian George[4], and Liwu Zhang[1,2]

[1]Shanghai Key Laboratory of Atmospheric Particle Pollution and Prevention, Department of Environmental Science and Engineering, Fudan University, Shanghai, 200433, P. R. China.
[2]Shanghai Institute of Pollution Control and Ecological Security, Shanghai, 200092, Peoples' Republic of China.
[3]Key Laboratory of Cluster Science, Ministry of Education of China, School of Chemistry and Chemical Engineering, Beijing Institute of Technology, Beijing 100081, P. R. China
[4]Univ. Lyon, Université Claude Bernard Lyon 1, CNRS, IRCELYON, F-69626, Villeurbanne, France.

Correspondence to: Liwu Zhang (zhanglw@fudan.edu.cn)

Abstract. Carbon dioxide is considered an inert gas that rarely participates in atmospheric chemical reactions. However, we show here that CO_2 is involved in some important photo-oxidation reactions in the atmosphere through the formation of carbonate radicals ($CO_3^{\cdot-}$). This potentially active intermediate $CO_3^{\cdot-}$ is routinely overlooked in atmospheric chemistry regarding its effect on sulfate formation. Present work demonstrates that SO_2 uptake coefficient is enhanced by 17 times on mineral dust particles driven by $CO_3^{\cdot-}$. It can be produced through two routes over mineral dust surfaces: i) hydroxyl radical + CO_3^{2-}; ii) holes (h^+) + CO_3^{2-}. Importantly, upon irradiation mineral dust particles are able to produce gas-phase carbonate radical ions when the atmospherically relevant concentration of CO_2 presents, therefore potentially promoting external sulfate aerosol formation and oxidative potential in the atmosphere. Employing a suite of laboratory investigations of sulfate formation in the presence of carbonate radical on the model and authentic dust particles, ground-based field measurements of sulfate and (bi)carbonate ions within ambient PM, together with density functional theory (DFT) calculations for single electron transfer processes in terms of $CO_3^{\cdot-}$-initiated S(IV) oxidation, a novel role of carbonate radical in atmospheric chemistry is elucidated.

1. Introduction

Atmospheric composition changes are subjected to highly reactive light-induced radicals, such as hydroxyl (·OH), hydroperoxyl ($HO_2\cdot$), or nitrate radicals ($NO_3\cdot$), which are able to alter not only compositions but also physical and chemical properties of particulate matter (Davis and Francisco, 2011; Platt et al., 1990; Prinn et al., 2001; Thompson, 1992). However, when atmospheric chemical reactions occur over nanometer-sized particles at ambient conditions, which creates a locally enriched aqueous medium of unique chemical activity, other radicals might likewise gain importance. The carbonate radical

($CO_3^{\cdot-}$) is typically such an active radical. The lifetime of $CO_3^{\cdot-}$ ranges from a microsecond to even a few milliseconds and its concentration can be two orders of magnitude higher than that of hydroxyl radicals over the water surface (Chandrasekaran and Thomas, 1983; Goldstein et al., 2001; Shafirovich et al., 2001; Sulzberger et al., 1997). In addition, the one-electron reduction potential of $E^0(CO_3^{\cdot-}/CO_3^{2-})$ couple is 1.78 V vs. NHE at neutral pH, leaving $CO_3^{\cdot-}$ a strong oxidant in aquatic chemistry (Bisby et al., 1998; Cope et al., 1973 ; Merouani et al., 2010). Previous studies concerning carbonate radical in aqueous media demonstrate that it reacts rapidly with some organic compounds with higher selectivity (Merouani et al., 2010), especially for those electron-rich compounds amines (Stenman et al., 2003; Yan et al., 2019). Also, it has been pointed out that the scavenging of hydroxyl radicals by (bi)carbonate species leads to the formation of $CO_3^{\cdot-}$ ions (Graedel and Weschler, 1981), which promotes the degradation of phenol (Xiong et al., 2016). Besides, a higher second order of rate constant, lying at 10^9 M^{-1} s^{-1}, has been reported for the reaction of $CO_3^{\cdot-}$ with porphyrins (Ferrer-Sueta et al., 2003), indicating that this radical ion has great oxidation capability that may trigger atmospherically relevant chemical reactions. However, it is only regarded as a marginal intermediate in tropospheric anion chemistry so far (Beig and Brasseur, 2000; Dotan et al., 1977; Graedel and Weschler, 1981; Lehtipalo et al., 2016) and its underlying role as an active oxidant for heterogeneous reaction in the atmosphere is barely explored. Very recently, our group observed the promotional effect of $CO_3^{\cdot-}$ on atmospheric nitrate formation (Fang et al., 2021). Motivated by this finding, attempts were made to further explore its role in other important atmospherically-relevant reactions.

It is well documented that sulfate (SO_4^{2-}) is also a key constituent of aerosols in the atmosphere (Huang et al., 2015; Su et al., 2016). It is able to serve as the precursors of efficient cloud condensation nuclei, with optical properties leading to a cooling effect (Wang et al., 2011). As a consequence, the mechanism aspect of secondary sulfate formation was the focus of numerous studies over the past decades (Hung et al., 2018; Stone, 2002; Zhang et al., 2015b). There is a consensus that high-valence sulfur (VI), produced from the oxidation of anthropogenic SO_2, is the dominant source for atmospheric secondary sulfate. However, a remarkable missing sulfate budget emerges for the atmospheric modeling, which underpredicts SO_4^{2-} by over 50 % (normalized mean bias) with respect to observational results when heterogeneous aerosol chemistry is not considered (Zheng et al., 2015). This indicates that the heterogeneous sulfate production pathway is a crucial process and exploring the unconsidered heterogeneous mechanism is very likely to narrow the gap between observations in lab studies, field measurements, and numerical modelings. However, due to the missing chemical mechanism that initiated fast SO_2 oxidation, atmospheric models fail to capture the key feature of atmospheric observations of high sulfate production (Wang et al., 2020). Consequently, there are unknown heterogeneous reaction pathways of significance and previously unconsidered promoters that have great potential to accelerate sulfate formation.

Due to the high stability of CO_2 under ambient conditions (Hossain et al., 2020), there are rare studies concerning the influence of CO_2 in atmospheric chemical processes (Deng et al., 2020; Liu et al., 2020a; Xia et al., 2021). CO_2 is demonstrated to form (bi)carbonate species over humidified dust particles (Baltrusaitis et al., 2011; Nanayakkara et al., 2014) and reduced to CO under solar illumination (Deng et al., 2020). However, its impact on atmospheric heterogeneous reactions remains poorly characterized. Our earlier laboratory study shows that CO_2 decreases the sulfate formation on aluminum

oxide particles in the dark (Liu et al., 2020b) while upon solar illumination its role in SO_2 oxidation over mineral dust surfaces is still an open question. In addition, carbonate salt is enriched in authentic dust aerosol (Cao et al., 2005) and reported to reach over 10 % wt. of Asian dust particles (McNaughton et al., 2009). It is generally accepted that CO_3^{2-} affects atmospheric chemistry and aerosol characteristics mainly through its intrinsic alkalinity, which buffers aerosol acidity and favors the sulfate formation (Bao et al., 2010; Kerminen et al., 2001; Yu et al., 2018). In fact, either CO_2 or carbonate salt is able to produce the active $CO_3^{\cdot-}$ under the ambient circumstance and increase the oxidative capacity in the atmosphere. Combined with our previous investigation of $CO_3^{\cdot-}$ (Fang et al., 2021), this radical ion is likely to be a driving force for fast SO_2 oxidation. However, to the best of our knowledge, no work has considered how and to what extent the carbonate radical influences SO_2 heterogeneous oxidation in the atmosphere.

In the current study, through laboratory studies, we presented that carbon dioxide and calcium carbonate, working as the precursor of carbonate radicals, extend their ability to accelerate sulfate formation over authentic particles in the atmosphere. Together with quantum chemistry calculations, a detailed molecular mechanism regarding a single electron transfer (SET) process between carbonate radical and sulfite ions is elucidated. Furthermore, ground-based observations validate some findings from the laboratory-based simulations.

2. Experimental methods

2.1 Laboratory Studies

A series of characterizations were initially performed to investigate the mineral dust of concern by using X-ray diffraction (XRD) and Raman technique. The heterogeneous reaction of SO_2 on mineral dust particles in the presence of CO_2 and carbonate species were then investigated by the *in situ* Fourier transform spectrum (DRIFTS), ion chromatography (IC), Raman, electron spin resonance (ESR), and nanosecond transient absorption spectroscopy (NTAS). Furthermore, we employed three types of authentic dust particles and four kinds of synthesized authentic simulants to probe the proposed scheme. Besides, the steady concentration of $CO_3^{\cdot-}$ ions in each reaction system was determined by High-Performance Liquid Chromatography (HPLC) using probe molecule aniline. All corresponding configuration setup, characterizations, and methodologies can be found in Supplement text 1, 2, 8-18, and Tables S1-S3, and Fig. S1-S12 and Fig. S15-S17. In terms of oxygen isotope experiments, more detailed procedures are available in Supplement, text 21.

2.2 Quantum Chemical Calculation

We employed density functional theory (DFT) calculations in the term of the single electron transfer (SET) process using Gaussian 09 package to investigate this novel route, detailed in Supplement text 19-20 and Fig. S13-S14.

2.3 Field Observations

Atmospheric aerosols were collected on the roof of our department using an 8-stage non-viable-cascade-impactor type sampler (TISCH TE Inc., USA), with sampling details shown in supplement Text 22 and daily variations of wind scales shown in Fig. S18. The concentration of water-soluble sulfate ion was by measured IC analysis while that of (bi)carbonate ions was determined by the ionization balance approach (Supplement text 23-24). The relationship between (bi)carbonate ions and sulfate ions during the daytime and nighttime hours were then determined.

3. Results and discussion

3.2.1 Accelerated sulfate production in the presence of carbonate.

The physico-chemical properties of employed mineral dust proxies were first characterized (Fig. S1), consistent with earlier studies (Balachandran and Eror, 1982; Shang et al., 2010; Su et al., 2008), and spectral irradiance of the solar simulator applied in the present study is well covered by natural sunlight (Fig. S2), as much as possible having experimental results from the lab simulate the real atmosphere. Upon irradiation, the sulfate yield on TiO_2-$CaCO_3$ mixture particles (50 wt. % $CaCO_3$), measured by IC, is significantly enhanced by 7 times and 23 times compared to that of pristine TiO_2 and $CaCO_3$ (Fig. 1a), respectively. In stark contrast, there is a negligible increase of sulfate production detected on the TiO_2-$CaCO_3$ mixture relative to that of pristine $CaCO_3$ and TiO_2 in dark experiments (Fig. 1a). While great discrepancies in sulfate yield between dark and irradiation experiments, it remains unclear for the role of carbonate salt in promoting sulfate formation. There is a prevailing view that neutralization of H_2SO_4 accounts for rapid SO_2 oxidation over carbonate salt particles, which needs careful consideration. Following this speculation, two types of mixtures TiO_2-$CaCO_3$ and TiO_2-CaO were employed. In the dark condition (Fig. S3), both TiO_2-CaO and TiO_2-$CaCO_3$ almost yield an identical concentration of sulfite and sulfate as they are likely to present similar physical and chemical properties, e.g. surface pH and neutralization capability. Once irradiated, TiO_2-$CaCO_3$ particles produce nearly two times of sulfate than TiO_2-CaO particles, along with a sharp decrease of S(IV) species on the surface of TiO_2-$CaCO_3$ surfaces (see additional discussion in the supplementary text 2). These results allow us to assert that the carbonate-containing system contains another important mechanism for sulfate generation beyond the production of an alkaline environment. Fig. 1b and 1c show the *in situ* diffuse reflectance infrared DRIFTS features of S(IV) and S(VI) species formed on theoretical and experimental TiO_2-$CaCO_3$ mixtures (wt./wt. = 50/50) upon irradiation for 90 min, respectively. The "theoretical" here is calculated based on the *in situ* DRIFTS of pristine TiO_2 and $CaCO_3$ through a simple linear superposition. These results suggest a synergistic effect presented in this mixture for sulfate formation under solar irradiation. In addition, a more evident fingerprint SO_4^{2-} feature (Dong et al., 2009; Yann Batonneau et al., 2008) monitored by Raman spectroscopy appears over TiO_2-$CaCO_3$ particles compared to pristine TiO_2 particles (Fig. S4), in good agreement with the IC analyses and *in situ* DRIFTS measurements. Combining DRIFTS experiments with the obtained calibration curve (Fig. S5), we estimated that the uptake coefficient of TiO_2-$CaCO_3$ mixture (50 wt. % $CaCO_3$) is increased

by about 17 times as compared to that of pure $CaCO_3$ or TiO_2 (Table S3). More importantly, upon irradiation SO_2 uptake coefficients for these dust proxies lie at the order of magnitudes of 10^{-4}, indicating that the photochemical pathway associated with carbonate species is likely a potential driving force to trigger fast SO_2 oxidation in the atmosphere.

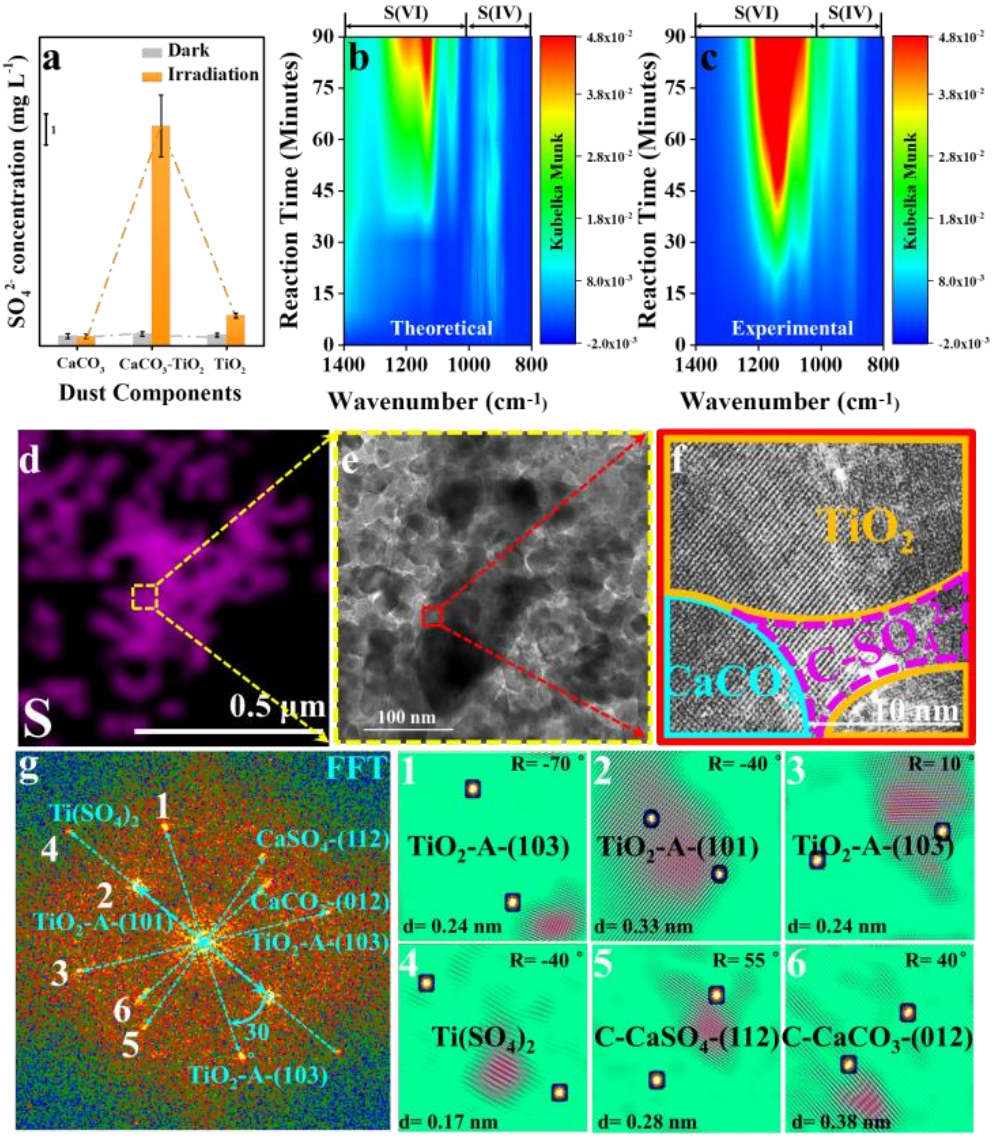

Figure 1. (a) Sulfate concentration quantified by IC on mineral dust particles after exposure to gaseous SO_2 under irradiation or dark for 30 min. *In situ* DRIFTS of S(IV) and S(VI) species yield on theoretical **(b)** and **(c)** experimental TiO_2-$CaCO_3$ mixtures (wt./wt. = 50/50) upon irradiation for 90 min. Reaction conditions: RH = 30 %, Light intensity (I) = 30 mW cm^{-2}, Total flow rate = 52.5 mL min^{-1} and SO_2 = 2.21×10^{14} molecules cm^{-3}. All spectra were processed by the Kubelka-Munk (K-M) algorithm. Noting that the production of sulfur species in theoretical TiO_2+$CaCO_3$ mixtures refer to 0.5 × K-M bands of sulfur species of TiO_2 + 0.5 × K-M bands of sulfur species of $CaCO_3$ while that for experimental TiO_2+$CaCO_3$ mixtures refer to 1 × K-M bands of sulfur species of TiO_2+$CaCO_3$ mixtures (wt./wt. = 50/50). **(d)** Energy Dispersive Spectroscopy (EDS) mapping of sulfur. **(e)** Selected HRTEM region containing a high density of sulfur for further observation and the red rectangle refers to the region shown in panel f. **(f)** The HRTEM image in high resolution with lattice fringes and **(g)** corresponding FFT power spectra, lattice indexing, and (1-6) inverse FFT analysis of lattice signal shown in panel g. In panel f, the term

C-SO_4^{2-} stands for crystalline SO_4^{2-}, i.e. $CaSO_4$ and $Ti(SO_4)_2$. Particles for the HRTEM measurement refer to TiO_2-$CaCO_3$ mixture particles upon exposure to the 4.42×10^{14} molecules cm^{-3} SO_2/N_2+O_2 for 60 min while other reaction conditions are as same as that of above sulfate quantification experiments.

High-resolution transmission electron microscopy (HRTEM) analysis of TiO_2-$CaCO_3$ particles after reaction, in combination with energy dispersive spectrometer mapping measurements of sulfur component, were conducted to investigate the synergistic effect between TiO_2 and carbonate ions (Fig. 1 d-f and Fig. S6). A region with a relatively high density of sulfur species was selected for further observation and the distribution of each component (Fig. 1g) was determined by fast Fourier transformation (FFT) and inverse FFT analyses of the selected HRTEM image in high resolution with lattice fringes shown in Fig. 1f. Observation of crystalline $Ti(SO_4)_2$ and $CaSO_4$ on the interface of TiO_2 and $CaCO_3$ components imply that the synergistic effect on sulfate production likely originates from interplays of those two types of components under solar illumination. We further assessed the importance of interfacial contact between TiO_2 and $CaCO_3$ in sulfate production by two synthesis approaches in which the interface abundance is modulated for comparison. Typically, a "grinding" method was used to make TiO_2-$CaCO_3$ mixture with compact contact between those two components, thus leading to a strong interaction. Meanwhile, the "shaking" method is designed to create a TiO_2-$CaCO_3$ mixture with weak interplay, leaving relatively fewer amounts of interfaces within the mixtures. The resulting mixing statuses of two samples meet our expectations, evidenced by the scanning electron microscope (SEM) technique (Fig. S7). IC quantification analysis suggests that particles with considerable junctions exhibit a more pronounced promotion for sulfate yield than those having relatively few junctions (Fig. S8). These results emphasize the importance of an indispensable interface connection between TiO_2 and $CaCO_3$ in fast production upon irradiation.

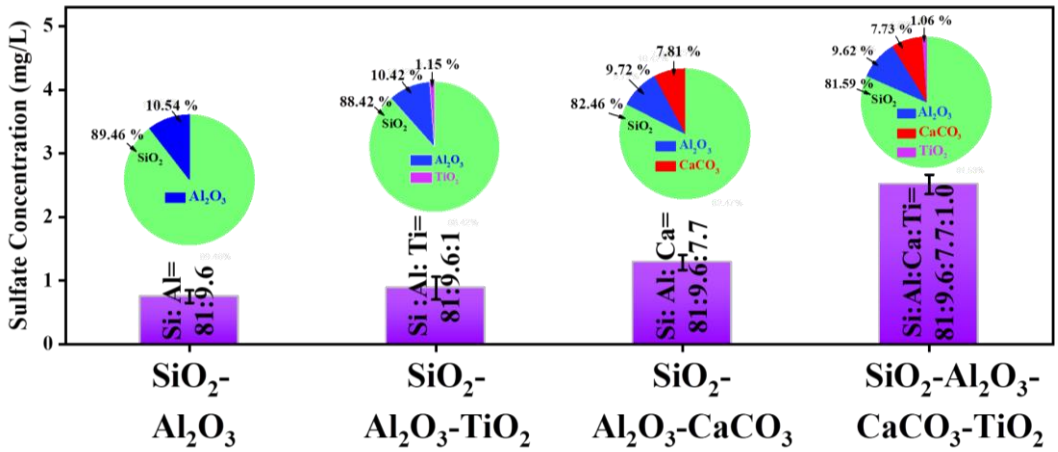

Figure 2. Sulfate concentration quantified by IC. Sulfate concentration was measured by IC on mineral dust simulants after exposure to gaseous SO_2 (2.46×10^{14} molecule cm^{-3}) under irradiation. Noting that SiO_2: Al_2O_3: $CaCO_3$: TiO_2 refers to the mass fraction ratios of the components in simulants. Experiments were all conducted at RH of 30 % and Light intensity (*I*) of 30 mW cm^{-2}.

The rapid SO_2 oxidation pathway was further probed by employing mineral dust simulants where two dominant crust constituents SiO_2 and Al_2O_3 were introduced into TiO_2-$CaCO_3$ particles to mimic the authentic mineral dust particles in the atmosphere, with specific component and corresponding ratio information shown in Table S1. It is worth mentioning that the determination of the ratio of each component in the simulants relies on the EDS mapping results of ATD particles. In Fig. 2, the introduction of TiO_2 components ($\approx$ 1 % wt.) into SiO_2-Al_2O_3 leads to 81.6 % enhancement of sulfate production while merely 24.8 % wt. increase of sulfate yield was observed once $\approx$ 8 % wt. of $CaCO_3$ was incorporated into SiO_2-Al_2O_3 dust particles. Surprisingly, mixing of $\approx$ 1 % mass fraction of TiO_2 and $\approx$ 8 % wt. of $CaCO_3$ into SiO_2-Al_2O_3 gives rise to a 235 % increase of sulfate formation relative to that of SiO_2-Al_2O_3. Hence, the observed synergistic effect on heterogeneous oxidation of SO_2 is likely to take effect in the atmosphere.

Fe_2O_3 is also one of the crucial components found in authentic mineral dust (El Zein et al., 2013), and it has been reported to produce ROS under solar irradiation (Li et al., 2019), thus likely involving the reaction mechanism proposed in this work. Similar to experiments using TiO_2+$CaCO_3$ mixture, alpha-Fe_2O_3+$CaCO_3$ are prepared by grinding alpha-Fe_2O_3 and $CaCO_3$. In Fig. S9a, our results show that alpha-Fe_2O_3 can not trigger fast SO_2 oxidation in the presence of carbonate ions upon irradiation, which is distinguished from results we derived from TiO_2+$CaCO_3$ mixture. This can be explained by the fact that Fe_2O_3 shows a lower redox activity relative to TiO_2 (Fig. S9b), where its strong redox capability essentially enables photo-induced electrons and holes to produce $O_2^{\cdot-}$ and $\cdot OH$ radical ions. In stark contrast, the valence band and conduct band of Fe_2O_3 lie at -0.18 and at 1.68 V vs. NHE (pH = 7), lower than the redox potential required for generating $O_2^{\cdot-}$, $\cdot OH$ as well as $CO_3^{\cdot-}$ (Li et al., 2016). Hence, no promoted sulfate production is seen for Fe_2O_3+$CaCO_3$ particles under irradiation. More discussion on the inconsistency between our study and the previous results regarding the response of SO_2 oxidation to solar irradiation can be found in supplementary text 3.

Overall, we show that upon irradiation atmospherically relevant content of TiO_2 (nearly 1 %) found in authentic dust simulants is able to interact with carbonate ions to launch a fast SO_2 oxidation channel, which is beyond the conventional regime of alkaline neutralization of H_2SO_4. Unlike TiO_2, alpha- Fe_2O_3 lacks the ability to initiate fast SO_2 oxidation by generating $CO_3^{\cdot-}$ due to its limited photo-chemical activity although ferric chemistry is important in secondary sulfate formation in the atmosphere (Sullivan et al., 2007; Yermakov and Purmal, 2003).

3.2.2 Accelerated sulfate production in the presence of CO_2.

Atmospheric CO_2 is also an important source of (bi)carbonate. Its influence on photochemical SO_2 uptake on mineral dust was thus studied. In the presence of atmospherically relevant CO_2 (9.83×10^{15} molecules cm^{-3}), sulfate yield was increased under irradiation as compared to CO_2-free case (Fig. 3a and b). We cautiously examined the buffering effect of formed (bi)carbonate on sulfate production by time-resolved DRIFTS spectra (Fig. 3c and d). CO_2 suppresses both S(IV) and S(VI) products under the dark. This observation implies that (bi)carbonate ions that evolve active intermediates upon irradiation

may be a plausible force to drive rapid sulfate formation rather than accumulating much more sulfur species through buffering effect. The reaction kinetics of SO_2 on mineral dust particles follows the pseudo-first-order, as evidenced by the SO_2 concentration dependence experiments (Fig. S10 a-f). Besides, a nearly 50 % increase of SO_2 uptake coefficient is observed for the mineral dust proxy TiO_2 after being exposed to 9.83×10^{15} molecules cm^{-3} (400 ppm) CO_2+SO_2/N_2+O_2 mixture.

As another step toward a real scenario in the atmosphere, experimental trials employing authentic dust particles, i.e. Arizona test dust (ATD), clays IMt-2 (Illite, Mont., USA), and K-Ga-2 (Kaolin, Georgia, USA), were implemented (Table S2). In Fig. 4, K-Ga-2 clay exhibits the most marked promotional effect on sulfate yield (by nearly 100 % increased sulfate production in the CO_2-involved case under irradiation). This correlates with its considerable TiO_2 contents (3.43 %) in the K-Ga-2 clay, in which active intermediates are readily evolved from TiO_2 and (bi)carbonate species upon irradiation. However, the promotional effect of CO_2 on sulfate production under irradiation is weak for IMt-2 (the content of $TiO_2 \approx 0.99$ %) and ATD (the content of $TiO_2 \approx 0.46$ %) as compared to K-Ga-2 particles. This may correlate to their higher mass fraction of alkaline earth metal oxide (denoted as A.E.), which enables dust particles to possess a large number of (bi)carbonate species in the natural environment where they have experienced long-term exposure to atmospheric CO_2 during the regional transport. Therefore, the aforementioned synergetic effect takes effect over IMt-2 and ATD particles even without exposure to CO_2 due to the presence of abundant carbonate formed, and a less evident increase of sulfate yield was thus observed.

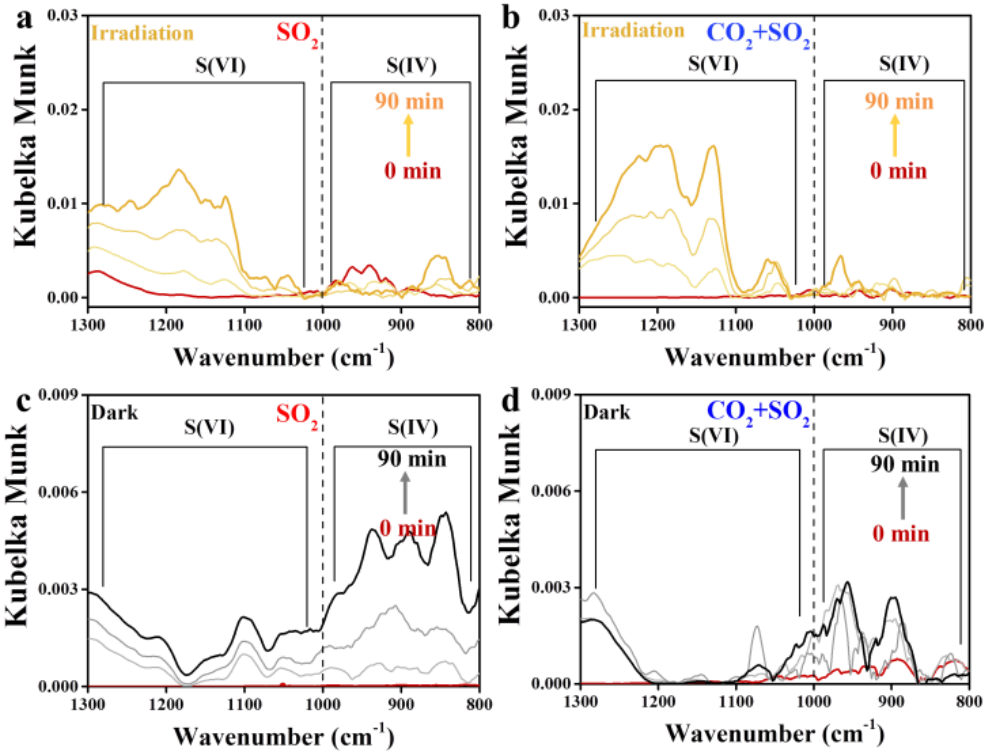

Figure 3. Time-resolved DRIFTS of S(IV) and S(VI) products over TiO_2 particles after exposure to SO_2/N_2+O_2 in the absence and presence of CO_2 upon irradiation (**a** and **b**) and those reactions under dark (**c** and **d**). Reaction conditions: RH = 30 %, Light intensity (I) = 30 mW cm^{-2}, total flow rate = 52.5 mL min^{-1} and SO_2 = 7.37×10^{13} molecules cm^{-3}.

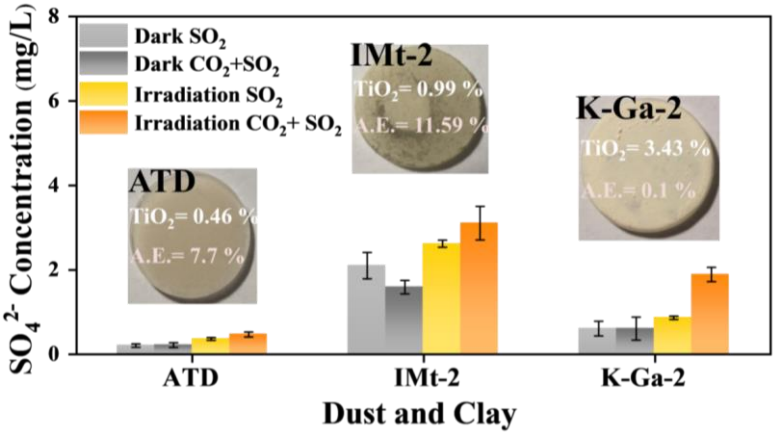

Figure 4. Laboratory studies of sulfate production on authentic dust and clay membranes under the dark and irradiation (30 mW cm^{-2}) upon exposure to 4.91×10^{14} molecules cm^{-3} SO_2/N_2+O_2 and 2.46×10^{18} molecules cm^{-3} CO_2+ 4.91×10^{14} molecules cm^{-3} SO_2/N_2+O_2 at RH of 30 % (total flow rate = 100 mL min^{-1}).

3.2.3 Reaction Mechanism.

The heterogeneous reaction of SO_2 on dust particles in the atmosphere is a complicated process, covering a series of reactions taking place through both homogeneous and heterogeneous ways. At a sufficiently low RH condition (normally below 10 % RH), water readily dissociates on the surface of metal oxide under ambient atmospheric conditions, where metal oxide surface is terminated by hydroxyl groups that hydrogen bond to adsorbed water molecules (Cwiertny et al., 2008). In this case, SO_2 oxidation over dust particles is dominated by the heterogenous pathway, where the resulting hydroxyl groups capture SO_2 in the gas phase first and then stabilize it as adsorbed $S(IV)_{ad}$. Afterward, $S(IV)_{ad}$ will be oxidized by oxidants in the atmosphere or photo-induced active intermediates produced from the dust surface upon irradiation. As the RH increases beyond 10 % -15 %, multilayer water coverage occurs, reaching approximately two monolayers at RH of 30 % (Mogili et al., 2006). Under these circumstances, the amount of water adsorbed onto the surface of the dust particles is believed to be sufficiently large that it is liquid-like in its physical and chemical properties (Cwiertny et al., 2008) (Peters and Ewing, 1997). In this work, heterogenous SO_2 oxidation over mineral dust proxies proceeds at the RH of 30 %, and two water layers absorb on dust particles. Thus, radical ions are expected to play a key role in fast SO_2 oxidation and mechanism studies performed in solution phase are persuasive to some extent.

Our preliminary sulfate quantification results (Fig. 1-4) suggest that the presence of (bi)carbonate ions under solar light contributes to increased sulfate yield. In our carbonate-containing reaction system, a plausible intermediate is the active

carbonate radical. They are readily produced via the following two pathways. First of all, carbonate anion can be directly oxidized by produced photo-induced holes (Eqs 2 and 3), as the redox potential of $CO_3^{\cdot-}/CO_3^{2-}$ is 1.78 V (vs NHE, at pH = 7), which is lower than the TiO_2 valence band (VB) potential of 2.67 V (vs NHE, at pH = 7) (Li et al., 2016; Xiong et al., 2016):

$$\text{Mineral dust} + h\nu \rightarrow h^+ + e^- \quad \text{(Eq. 1)}$$

$$h^+ + CO_3^{2-} \rightarrow CO_3^{\cdot-} \quad \text{(Eq. 2)}$$

In the second pathway, carbonate radicals evolve through the reaction of (bi)carbonate anion with formed hydroxyl radicals ·OH over mineral dust surfaces (Zhang et al., 2015a) (Eqs 3 and 4).

$$h^+ + H_2O_{ad} \rightarrow \cdot OH + H^+ \quad \text{(Eq. 3)}$$

$$\cdot OH + HCO_3^-/CO_3^{2-} \rightarrow CO_3^{\cdot-} + H_2O/OH^- \quad \text{(Eq. 4)}$$

The above assumptions are supported by nanosecond transient absorption spectra (NTAS), in which signal (ΔOD) of carbonate radical $CO_3^{\cdot-}$ at 600 nm (Bhattacharya et al., 1998) only emerged for dust suspension containing (bi)carbonate species (Fig. 5a). A promoted degradation of aniline in TiO_2 suspension due to the presence of carbonate ions presents additional evidence of the formation of active $CO_3^{\cdot-}$ ions and strengthened oxidation capability of TiO_2 (Fig. S11, see additional discussion in supplementary text 4). The $CO_3^{\cdot-}$-induced chemistry was further evidenced by ·OH scavenging experiments using tertiary Butyl Alcohol (TBA) and isopropanol (i-PrOH) as they show lower reaction rates with $CO_3^{\cdot-}$ ($k_{CO_3^{\cdot-},\text{i-Pr0H}} < 4.0 \times 10^4$ M^{-1} s^{-1} and $k_{CO_3^{\cdot-},\text{TBA}} < 1.6 \times 10^2$ M^{-1} s^{-1}) relative to that with ·OH ($k_{\text{i-PrOH}\sim\cdot\text{OH}} < 1.9 \times 10^9$ M^{-1} s^{-1} and ($k_{\cdot\text{OH,TBA}} = 6 \times 10^8$ M^{-1} s^{-1}) (Buxton et al., 2009; Liu et al., 2015) (Liu et al., 2015) (Li et al., 2020). Tertiary Butyl Alcohol (TBA) sharply decreases the yield of sulfate on TiO_2 surface by nearly 70 %, with sulfite ions being the dominant sulfur species (Fig. S12). Meanwhile, a significant loss of sulfate yield when TiO_2 suspension was added with i-PrOH (Fig. 5b). This is in strong contrast to the result of a carbonate-involved system where the reactivity is sustained, i.e., carbonate radicals offer an alternative reaction pathway for SO_2 oxidation. This is plausible since the carbonate ions are excellent ·OH scavenger, and $CO_3^{\cdot-}$ becomes predominant species at a relatively strong alkaline aqueous-like environment in the presence of carbonate salt. This is supported by the previous work (Sun et al., 2016), in which adding 0.1 M of $NaHCO_3$ into the UV/H_2O_2 system (H_2O_2 = 0.3 mM) were sufficient to suppress ·OH concentration to around 10^{-15} M, creating a carbonate radical dominated reaction system ([$CO_3^{\cdot-}$] = 8.64 × 10^{-12} M). In our supplementary experiments (Fig. S11), 0.2 M of carbonate salt was employed, and the reaction rate of CO_3^{2-} with ·OH is nearly two orders of magnitude higher than that of HCO_3^-, thus giving rise to carbonate radical being the substitute of hydroxyl radical in the reaction. The above results suggest that ·OH is a major contributor to sulfate yield on TiO_2 particles in the absence of carbonate ions while $CO_3^{\cdot-}$ ions dominate SO_2 oxidation over carbonate-containing dust particles upon irradiation. In addition to experimental investigations, the carbonate radical formation process is proved to be thermodynamically favorable, supported by density functional theory (DFT) calculations (Fig. S13).

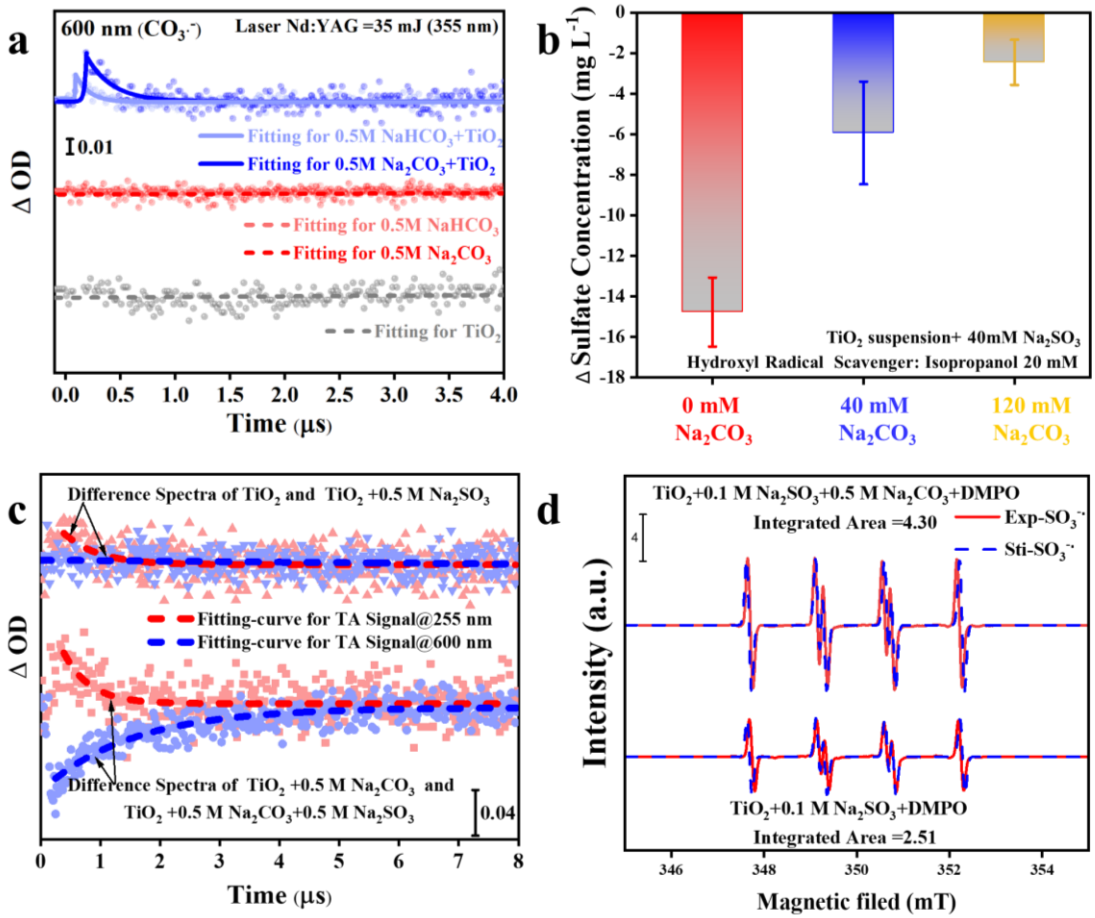

Figure 5. (**a**) Single-wavelength transient absorption spectra of various aqueous solutions. (**b**) Sulfate formation change $\Delta(SO_4^{2-})$ determined by different sulfate concentrations with and without the addition of isopropanol as hydroxyl radical scavenger. (**c**) The difference in transient absorption kinetics of sulfite radical and carbonate radical at the various aqueous solutions and their corresponding growth-decay fit curves. ΔA-signal was recorded at 255 and 600 nm after pulsed 355 nm laser excitation. (**d**) ESR spectrometry of [DMPO–$SO_3^{\cdot-}$] intermediate formed in a solution of d TiO_2 (3mg~4 mL) + 0.1 M Na_2SO_3 and TiO_2 (3mg~4 mL) + 0.5 M Na_2CO_3 + 0.1 M Na_2SO_3. For clarity, the integrated areas of ESR profiles were also presented for direct comparison. Exp. and Sti. stand for experimental results and corresponding fitting results using software Isotropic Radicals.

On the other hand, the previous studies (Chameides and Davis, 1982; Das, 2001; Neta and Huie, 1985) agree with the key role of sulfite radical ($SO_3^{\cdot-}$) in rapid sulfate production in an aqueous medium, and the present reaction system creates a localized environment where $SO_3^{\cdot-}$ can be readily produced from the TiO_2 and S(IV) species upon solar illumination (Salama et al., 1995). Consequently, probe light of NTAS at wavelength 255 nm (ascribed to sulfite radical) and 600 nm (ascribed to carbonate radical) were simultaneously monitored (Ghalei et al., 2016; Goldstein et al., 2001; Hayon et al., 1972). A weak signal of sulfite radical was observed in the system of TiO_2+Na_2SO_3 suspension under irradiation (Fig. 5c). On the contrary, the sulfite radical signal is strengthened after the introduction of carbonate ions into the TiO_2+Na_2SO_3

suspension, along with a significant decrease of signal for carbonate radical. ESR data (Fig. 5d) further confirms the increase of $SO_3^{\cdot-}$ after 2 min UV irradiation in the presence of carbonate ion. Based on the above results, one may deduce that the interplay between carbonate radical and sulfite ions is a crucial step giving rise to the increased $SO_3^{\cdot-}$ which is responsible for rapid SO_2 oxidation through chain propagation reactions (Deng et al., 2017). Nevertheless, there are two possibilities that might explain the aforementioned interaction. One is the oxygen transfer and the other route is electron transfer, which needs further clarification.

We first examined the oxygen transfer path through ^{18}O isotope labeling experiments. TiO_2 particles were initially exposed to $C^{16}O_2/N_2$ and $C^{18}O_2/N_2$, followed by the exposure of SO_2/N_2+O_2 under irradiation (Fig. 6a). Bidentate carbonate band centered at 1573 cm^{-1} appears after the introduction of $C^{16}O_2/N_2$, while this band shifts to 1558 cm^{-1} when $C^{18}O_2/N_2$ is introduced, indicating the incorporation of ^{18}O into bidentate carbonate species, in good agreement with the previous report (Liao et al., 2002). However, no shift of IR features at 1269, 1219, and 1159 cm^{-1}, assigned to (bi)sulfate species on TiO_2 particles, were observed throughout the reaction. This implies that the oxygen transfer path does not account for the rapid SO_2 oxidation on particles of concern.

In light of the above analysis, the electron transfer might be a plausible pathway to explain the fast oxidation within the reaction system. DFT calculations provide an accessible approach to study the electron transfer pathway. The result in Fig. 6b shows $SO_3^{\cdot-}$ formation is a SET process of $CO_3^{\cdot-}$ and SO_3^{2-}, where O atom in SO_3^{2-} transfers an electron to O atom in $CO_3^{\cdot-}$ to form $SO_3^{\cdot-}$ and CO_3^{2-}. This SET reaction is a thermodynamically favorable process, with the difference of Gibbs free energy between reactant and product lying at -24.09 kcal mol^{-1}. However, we noted that the insufficient O_2 supply in aqueous media may be an underlying constraint to the proposed $CO_3^{\cdot-}$-initiated SO_2 oxidation pathway. Hence, we estimated both oxygen consumption and supply rates, and oxygen supply flux can be several orders of magnitude larger than corresponding consumption (see additional details in the supplementary text 5). Therefore, oxygen is sufficient in the reaction, allowing the considered chain reactions to continually proceed. Taken above results and discussions together, the following reactions are proposed accordingly (Eqs. 5-8):

$$CO_3^{\cdot-} + SO_3^{2-} \rightarrow CO_3^{2-} + SO_3^{\cdot-} \quad \text{(Eq. 5)}$$

$$SO_3^{\cdot-} + O_2 \rightarrow SO_5^{\cdot-} \quad \text{(Eq. 6)}$$

$$SO_5^{\cdot-} + SO_3^{2-} \rightarrow SO_4^{\cdot-} + SO_4^{2-} \quad \text{(Eq. 7)}$$

$$SO_4^{\cdot-} + SO_3^{2-} \rightarrow SO_4^{2-} + SO_3^{\cdot-} \quad \text{(Eq. 8)}$$

Another important issue needs to be addressed as well. $SO_3^{\cdot-}$ can also be formed via the conventional reaction of ·OH and SO_3^{2-} (Eqs. 9) and this process is also considered.

$$\cdot OH + SO_3^{2-} \rightarrow SO_3^{\cdot-} + OH^- \quad \text{(Eq. 9)}$$

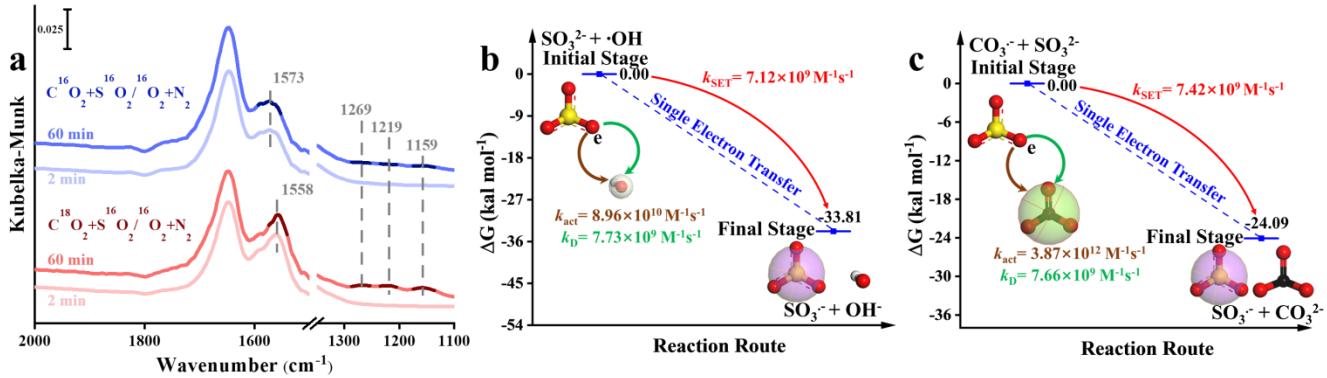

Figure 6. (**a**) *In situ* DRIFTS of heterogeneous reaction of SO_2 on the TiO_2 particles for 2 and 60 min after being exposed to $C^{16(18)}O_2/N_2$ for 20 min under irradiation. (**b**) Reaction pathway of interaction between hydroxyl radical (·OH) and sulfite (SO_3^{2-}) and (**c**) Interaction between carbonate radical ($CO_3^{\cdot-}$) and sulfite (SO_3^{2-}) through the SET process at the CCSD (T)-F12/cc-PVDZ-F12//M06-2X/6-311++G (3df, 3pd) level and ΔG_0^{SET} represents the difference in Gibbs free energy between reactant and product. The white, black, yellow, and red spheres represent H, C, S, and O atoms, respectively. In order to visualize the variation of surface products in oxygen isotope experiments (panel a), DRIFTS features of these concerned species were plotted in dark colors. For interpretation of the references to color in the legends of panels b and c, the reader is referred to the Web version of this article.

In this SET process, electron donor SO_3^{2-} reacts spontaneously with electron acceptor ·OH (Fig. 6c) and the calculated activation free energy barrier $\Delta G^{\neq}_{SET}$ for this SET reaction is 2.50 kcal mol^{-1}. Hence, the reaction process of ·OH with SO_3^{2-} is diffusion-controlled, and the total rate constant k_{SET-2} was calculated to be 7.12×10^9 M^{-1}s^{-1}. In comparison, the rate constant k_{SET-1} of the diffusion-controlled SET process for $CO_3^{\cdot-}$ and SO_3^{2-} was estimated to be 7.42×10^9 M^{-1}s^{-1}. Despite a slight net increase of the rate, the distinguishable concentration of $CO_3^{\cdot-}$ and ·OH should also be taken into account for the rate comparison in varied reaction paths. To visualize the difference, relative rates were calculated according to Eq. 10:

$$r=\frac{v_{CO_3^{\cdot-}+SO_3^{2-}}}{v_{\cdot OH+SO_3^{2-}}}=\frac{k_{SET-1}[CO_3^{\cdot-}][SO_3^{2-}]}{k_{SET-2}[\cdot OH][SO_3^{2-}]} \quad \text{(Eq.10)}$$

Where r is the ratio of two reaction rates, $[CO_3^{\cdot-}]$, $[SO_3^{2-}]$, and [·OH] refer to the concentration of corresponding reactants. Previous literature suggests the concentration of carbonate radicals is able to show two orders of magnitude higher than that of hydroxyl radical at the surface of the water under solar irradiation (Chandrasekaran and Thomas, 1983; Goldstein et al., 2001; Shafirovich et al., 2001). An aqueous medium that attaches to particle surfaces offers an ideal environment for accumulating carbonate radicals. Consequently, concentrations of $CO_3^{\cdot-}$ and ·OH were set at the range from 1.0×10^{-10} to 1×10^{-12} mol L^{-1} and from 1.0×10^{-12} to 1×10^{-14} mol L^{-1} (Sulzberger et al., 1997) and r value could thus reach to 1.04×10^4 at most (Fig. S14). As a result, we speculated that the formation pathway of $SO_3^{\cdot-}$ via interaction between $CO_3^{\cdot-}$ and SO_3^{2-} is a more effective route, corresponding well with experimental results.

In addition to the pathway launched by photo-generated holes, we also considered the sink of photo-generated electrons. In our reaction system, O_2 is believed to be an electron trap and produce the superoxide radical ions ($O_2^{\cdot-}$), which is reported to play a non-negligible role in sulfate formation (Shang et al., 2010) and should be taken into account to give a whole picture of reaction scheme in triggering sulfate formation on the surface of TiO_2-containing mineral dust particles. *p*-benzoquinone is a commonly-used $O_2^{\cdot-}$ scavenger for trapping the $O_2^{\cdot-}$ radical ions (Yan et al., 2018). Our supplementary data shows that adding an excess amount of *p*-benzoquinone into TiO_2 particles reduces the sulfate yield by 32 % along with the appearance of sulfite ions over TiO_2 particles upon exposure of SO_2 (Fig.S12). Notably, the decrease in sulfate yield by around 30 % in the presence of $O_2^{\cdot-}$ scavenger *p*-benzoquinone is almost complementary to that added with ·OH scavenger using TBA (70 %), pointing toward a minor sulfate formation pathway contributed by $O_2^{\cdot-}$ relative to the major pathway by $CO_3^{\cdot-}$ when carbonate ions are presented to efficiently capture ·OH ions. Following Shang's work (Shang et al., 2010), $O_2^{\cdot-}$ involved SO_2 oxidation can be given as Eqs. 11-13:

$$e^- + O_2 \rightarrow O_2^{\cdot-} \quad \text{(Eq.11)}$$

$$SO_2 + O_2^{\cdot-} \rightarrow SO_3 + O^{\cdot-} \quad \text{(Eq.12)}$$

$$SO_3 + H_2O \rightarrow H_2SO_4 \quad \text{(Eq.13)}$$

Where intermediates SO_3 formed via the interaction between SO_2 and $O_2^{\cdot-}$ subsequently couple with water molecules to produce sulfate species as a final product. pH is an important factor within aqueous chemical reaction processes and is likely to alter the dominated regime for sulfate production. Yet so far adjusting the pH of particle surfaces is quite tough, and exploring the role of dust surface pH in the reactivity of $CO_3^{\cdot-}$ is not easily achieved. Notwithstanding, the increase of pH in TiO_2 suspension was observed to promote the production of $CO_3^{\cdot-}$, further strengthening the oxidation capability of dust particles (Fig. S11). In contrast, decreasing pH is expected to reduce the yield of $CO_3^{\cdot-}$ since the reaction rate of CO_3^{2-} with ·OH is nearly two orders of magnitude higher than that with HCO_3^-. On this basis, the question arises whether the surface pH of mineral dust can be sustained to maintain fast SO_2 oxidation triggered by $CO_3^{\cdot-}$ in the typical lifespan of mineral dust.

Considering this, we thus plotted the heterogeneous sulfate production over TiO_2 and TiO_2+$CaCO_3$ particles versus equivalent exposure time (Fig. S15). Clearly, the sulfate yield builds up steadily during the two-week equivalent exposure time (see a more detailed discussion on determining equivalent exposure time in supplementary text 6), suggesting that the regime of $CO_3^{\cdot-}$ initiated SO_2 oxidation over TiO_2 and TiO_2+$CaCO_3$ particles are slightly affected by the possible decrease of surface pH due to accumulation of sulfate production over entire reaction course. In the atmosphere, the lifetime of mineral dust particles ranges from several days to weeks (Bauer and Koch, 2005), and the equivalent exposure time considered in this study (nearly 2 weeks) falls right within the characteristic lifespan range of mineral dust particles. This leads us to deduce that persistent growth of sulfate shows a negligible effect on $CO_3^{\cdot-}$ initiated SO_2 oxidation scheme proposed in this work.

Additionally, dust particles are reported to eject the radical ions from the surface under solar light irradiation, showing a non-negligible contribution to sulfate aerosol formation (Chen et al., 2021; Dupart et al., 2012), as described as:

Mineral Dust + $h\nu$ → ROS (g) (Eq.14)

ROS (g)+ humidified Air+ SO_2→Sulfate(g) (Eq.15)

Where ROS (g) stands for the active intermediates in the gas phase. Over 400 ppm of CO_2 is universal in the atmosphere, and it is expected to form (bi)carbonate ions once enters into the atmospheric aqueous media such as aerosol water, cloud droplets as well as fog environment. Bi(carbonate) ions are then prone to react with hydroxyl radical ions to form carbonate radicals. Following this line of reasoning, we attempt to monitor the plausible gas ROS species that are formed in the presence of CO_2 (see a detailed discussion about the measurement approach and experimental setup in supplementary text 7 and Fig. S16).

When CO_2 (atmospheric relevant concentration) is introduced into the homemade flow-cell chamber, with the intervening gap between TiO_2-coated film and probe molecule solution fixing at nearly 2 mm, and the short distance of which allows possible gaseous ROS to diffuse and react with aniline molecular (None, 2013). An increased degradation rate of aniline was seen, which can be attributed to the generation of active carbonate radical ions (Fig. S17). The maximum concentration of steady-state $CO_3^{\cdot-}$ radical ions supplied by partition processes between gas phase and solid-liquid phases (humified dust particles) was determined to be 1.39×10^{-13} M for TiO_2+Air+CO_2 system, which is over one order of magnitudes higher than that of ·OH for TiO_2+Air+system (2.15×10^{-15} M). This observation matches with the earlier study where the concentration of carbonate radical can be two orders of magnitudes than ·OH over the water surface (Sulzberger et al., 1997).

The above results suggest that the photochemistry that involves carbonate ions, more precisely $CO_3^{\cdot-}$ radical, increases sulfate formation. This finding broadens the prevailing view that acceleration of SO_2 oxidation over the carbonate salt is merely due to the favorable neutralization of H_2SO_4 over an alkaline surface. To be important, upon irradiation active component TiO_2 in mineral dust produce carbonate radical in the gas phase when $CO_3^{\cdot-}$ precursor CO_2 is presented, therefore potentially promoting sulfate aerosol formation in the atmosphere. Overall, it could be speculated that carbonate radical ions strengthen the oxidative capability of TiO_2-containing mineral dust particles, and consequently accelerate SO_2 oxidation.

3.2.4 Field Measurements of Sulfate and (Bi)carbonate Ions.

Complement field sampling and analysis were further conducted to examine our hypothesis that intermediates $CO_3^{\cdot-}$ may play role in secondary sulfate formation in the atmosphere. We first considered the meteorological condition wind speed, which is an important parameter determining whether the local chemical process gains importance in affecting secondary sulfate formation. Meteorological information was collected from the open-access database (https://www.aqistudy.cn/). During the sampling period, the wind scale mainly varies from 0 to 1, corresponding to the wind speed ranging from 0 to 1.5 m s^{-1} (Fig. S18). All plots shown in Fig. S18 give rise to a statistical wind speed of 0.76 ± 0.73, which represents the weak dispersion of pollutants at low wind speed (not exceeding 2.5 m s^{-1})(Witkowska et al., 2016; Wu et al., 2020), indicating that local source is a dominant contributor to local air pollution.

It is generally accepted that under stagnant meteorological conditions (wind speed < 1.5 m s^{-1}), for the coarse-mode (2.5 μm ~ 10 μm) of sulfate, the heterogeneous reaction of SO_2 on the dust surfaces is believed to be a major contributor (Liu

et al., 2017). This correlates to the fact that a large mass fraction of mineral dust is abundant in coarse-model particulate matter (PM) (Fang et al., 2017; Miller-Schulze et al., 2015), in which TiO_2 was found at mass mixing ratios ranging from 0.1 to 10 % depending on the exact location where particles were uplifted (Chen et al., 2012; Hanisch and Crowley, 2003). Therefore, PM with relatively larger size dimensions is expected to contribute to secondary sulfate formation via heterogeneous reactions, which is supported by the recent field study where carbonate fraction of coarse PM is evidenced to promote secondary sulfate production (Song et al., 2018). Considering this, rather than determine the concentration of water-soluble ions in all stages, more attention was paid to PM collected in stages 1-4 (particles with their dimension ⩾ 3.3 μm). As (bi)carbonate ions are known as key precursors in producing $CO_3^{\cdot-}$ and accelerate sulfate formation, quantifications of those relevant water-soluble ions were thus conducted (supplement text 23 and 24).

We further considered the relationships between sulfate ions and (bi)carbonate ions by means of linear regression analysis. However, under the low wind speed (0.76 ± 0.73), correlation coefficients R^2 obtained for the relationship between bi(carbonate) and sulfate ions are not promising, 0.56 (sulfate vs carbonate) and 0.61 (sulfate vs bicarbonate) for $PM_{3.3}$-$PM_{9.0}$ during daytime hours. A plausible explanation is that although less significant, local primary emission source also brings bias and uncertainty to the correlation analysis. Shanghai is a coastal city, and sulfate species such as K_2SO_4 and Na_2SO_4 from the sea salt contribute to the local sulfate emission as well (Long et al., 2014). On the other hand, this novel SO_2 oxidation channel is in the infant stage, and only active mineral dust components have been considered in this work whereas other components found in the coarse mode of PM such as organic matter, elemental carbon as well as sea salt (Cheung et al., 2011) are likely to involve this mechanism and alter the response of sulfate yield to SO_2 heterogeneous uptake. In addition, the water-soluble ions determined in these samples (relatively small size) may not come from the net contribution of heterogenous reaction processes in absolute day-time and night-time periods. Some of the undesired processes that take place during day(nigh)-night(day) shifts may also contribute to the prodcution of sulfate ions in separate sampling hours, thus reducing the correlation coefficients.

For those large particles (LP), that refer to the particles with a diameter large than 9 μm in this work, sulfate ions show a rather weak or even no correlation to (bi)carbonate ions during the night-time and day-time hours (Fig. S19). This is likely due to the short lifetime of LP. Generally, the aerosol lifetime is on the order of less than an hour to days (Koelemeijer et al., 2006), highly depending on particle size. For example, the lifetime of PM_{10} ranges from minutes to hours, and its travel distance, in general, is less than 10 km (Agustine et al., 2018). As a consequence, secondary sulfate formation through chemical reaction over LP is not significant with respect to *in situ* emissions. When PM downsizes to 2.5 μm, $PM_{2.5}$ has a lifetime prolonged to nearly one day or longer (Liu et al., 2020b). Therefore, $PM_{3.3}$-$PM_{9.0}$ are expected to have a relatively long lifetime, on the order of several hours, which enables the heterogeneous reaction process to become a more important contributor to overall sulfate ions measured in $PM_{3.3}$-$PM_{9.0}$ than that in $PM_{\geq 9.0}$. This is supported by our observations where during the daytime hours the correlation coefficients for $PM_{3.3}$-$PM_{9.0}$, i.e. 0.56 (sulfate vs carbonate) and 0.61 (sulfate vs bicarbonate), are higher than that of $PM_{\geq 9.0}$, i.e. 0.489 (sulfate vs carbonate) and 0.36 (sulfate vs bicarbonate), respectively.

Similarly, higher correlation coefficients are also observed for $PM_{3.3}$-$PM_{9.0}$ than $PM_{\geq 9.0}$ in the sample collected during the nighttime periods.

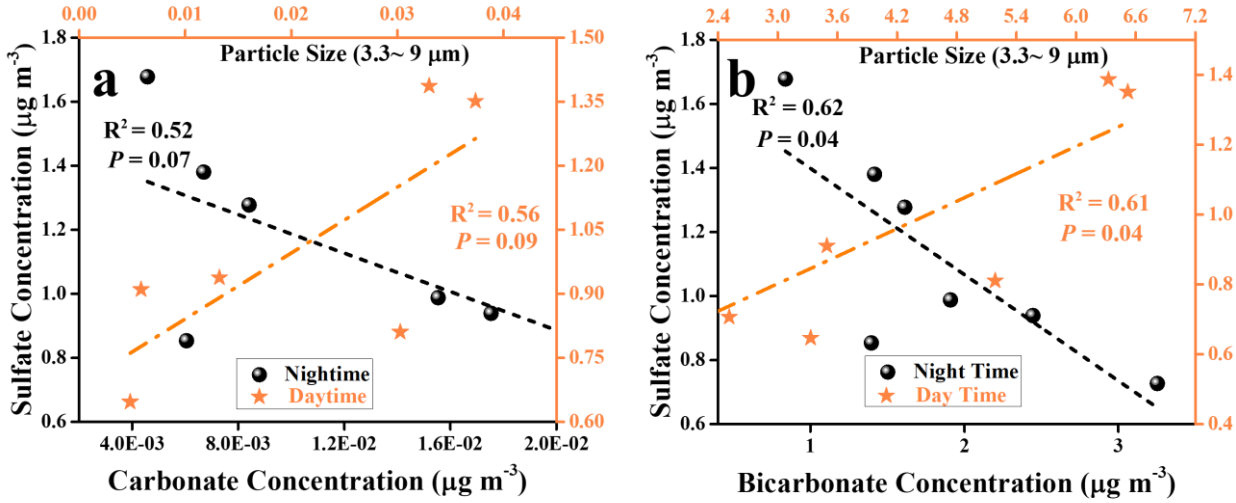

Figure 7. Field observation for the relationship between carbonate and sulfate ions during day-time and night-time hours. Linear relationship analyses for measured sulfate ions and estimated carbonate ions (**a**) and for measured sulfate ions and estimated bicarbonate ions (**b**) during the day-time and night-time hours, with particle sizes of PM ranging from 3.3 to 9 μm.

While we note that the correlation coefficients between sulfate and (bi)carbonate are not promising in this work, ground-based field measurements of sulfate and (bi)carbonate ions shed light on their distinct correlations during the daytime and nighttime hours. In Fig. 7 and Fig.S19, the negative correlations between the mass concentrations of sulfate ions and (bi)carbonate ions are observed in the nighttime hours, consistent with the suppression of sulfate formation by CO_2 in the dark experiments. This is also supported by our previous lab study where CO_2-derived (bi)carbonate species are demonstrated to block the active sites for yielding sulfate over mineral dust proxy aluminum oxide (Liu et al., 2020a). Instead, positive correlations were seen for those ions within PM sampled during the daytime hours regardless of size ranges and carbonate types (HCO_3^-/CO_3^{2-}). This matches with the scenarios in which sulfate production upon irradiation in the presence of (bi) carbonate ions is increased over both model and authentic dust particles. Except the case (nighttime period, size larger than 9 μm), most of the significance *P* values for their correlations were smaller than 0.1, with significance *P* values below 0.5 determined for bicarbonate vs sulfate, implying the plausible underlying connection between sulfate and (bi)carbonate ions. In fact, preceding ground-based observations of highly correlated relationship between Ca^{2+} and SO_4^{2-} water-soluble ions (Liu et al., 2020b) during the carbonate-enriched dust storm episodes, together with persistent reports on the significant role of photochemical channels in increasing the sulfate concentration during the daytime (Kim et al., 2017; Wei et al., 2019; Wu et al., 2017) indirectly reflects the possibility of accelerated SO_2 oxidation triggered by photo-generated active intermediates associated with carbonate species.

Overall, this is the first time that relationships between those ions are explored separately in these two periods. Taken together, carbonate radical is likely to promote sulfate production in the atmosphere during daytime hours. Detailed and systematic SO_2 oxidation channel triggered by $CO_3^{\cdot-}$ needs further investigations to enable a better interpretation of correlations between these inorganic ions at the given meteorological conditions of sampling and physico-chemical properties of PM.

4. Conclusion

On the basis of the experimental and theoretical results derived from this work, we for the first time propose a novel reaction channel for fast SO_2 oxidation over mineral dust particles due to the formation of carbonate radical ions. A schematic chart for the sulfate formation in the presence of carbonate radicals upon solar irradiation or bi(carbonate) ions under dark conditions is summarized and elucidated in Fig. 8. During the night-time hours at 298 K (ambient temperature) CO_2-derived (bi)carbonate species are prone to have a slightly negative effect on sulfate formation due to the competitive adsorption between CO_2 and SO_2. For alkaline carbonate salt, it favors sulfate formation through the neutralization process. On the other hand, during the day-time hours, both CO_2-derived (bi)carbonate species and carbonate salt work as the precursor of $CO_3^{\cdot-}$, which promotes sulfate formation. Especially, uptake coefficients for carbonate salt containing mineral dust can be increased by 17 times, which is more pronounced than the increase due to the neutralization regime in the dark condition. Consistent with the findings reported in the earlier studies (Chen et al., 2021; Dupart et al., 2012), we observed the production of gas-phase $CO_3^{\cdot}$ ions when mineral dust particles are irradiated in the presence of CO_2 (atmospherically-relevant concentration 400 ppm). This observation implies that the increased sulfate yield in part comes from promoted gas-phase secondary sulfate aerosol triggered by $CO_3^{\cdot-}$ (g).

By means of ROS scavenger experiments, direct observation of carbonate radical using NTAS analysis, oxygen isotope assay, ESR spectra as well as DFT calculations, $CO_3^{\cdot-}$-initiated S(IV) oxidation involving single electron transfer process are elucidated. While carbonate radical ions are mainly responsible for rapid sulfate formation, superoxide radical ions are likely to serve as a minor pathway over TiO_2-containing mineral dust particles. In addition, a weak correlation between sulfate ions and (bi)carbonate ions observed for $PM_{3.3}$-$PM_{9.0}$ in this work correlates to non-chemical primary emission and complicated nature of $CO_3^{\cdot-}$ regime of sulfate production in the atmosphere. Nevertheless, complement field sampling of ambient PM and analysis of sulfate and (bi)carbonate ions in this study unfold their distinct correlations during the daytime and nighttime hours, these two tendencies of which agrees with the experimental observations.

In this work, only atmospheric secondary sulfate formation was considered, whereas the oxidation of primary organic species yet has not been investigated. In fact, carbonate radical ions are prone to rapidly react with electron-rich organics amines (Stenman et al., 2003; Yan et al., 2019) as well as phenol (Busset et al., 2007; Xiong et al., 2016), and it may potentially serve as the key oxidants that drive the fast formation of SOA in the atmosphere. Besides, observation of strengthened photochemistry launched by carbonate radicals suggests that such chemistry may be amplified on

atmospherically relevant reactions that occur in cloud droplets as well as fog water where they often contain hydroxyl radicals and water-soluble (bi)carbonate ions.

To be important, carbonate radical ions are observed to be formed in the gas phase in the atmospherically relevant CO_2 concentration (400 ppm) when mineral dust proxies are irradiated. This will help the formation of external sulfate aerosol formation. Since both sulfate aerosol and CO_2 are well known to affect the radiation budget and solar energy balance on the earth (Cheung et al., 2011; Möller, 1964), their overall influence on the global climate considering the increased yield of sulfate aerosol triggered by CO_2, the precursor of carbonate radical, needs further investigation. Therefore, our study highlights the necessity for a comprehensive understanding of the $CO_3^{\cdot-}$ relevant chemistry in the underlying impacts of fine PM concentration, human health, and climate. All these assumptions need to be investigated in further detail. This study provides the first indication that carbonate radical not only plays a role as a marginal intermediate in tropospheric anion chemistry but also as a strong oxidant for surfacial processing of trace gas in the atmosphere.

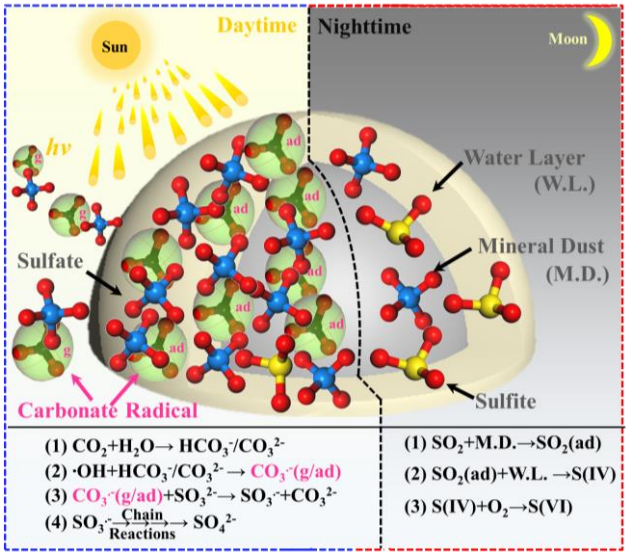

Figure 8. Schematic of the sulfate formation in the presence and absence of carbonate radical. Noting that g and ad represent gas-phase and adsorbed carbonate radical ions, respectively.

Data availability. The data that support the results are available from the corresponding author upon request.

Author contributions. Y.L., Y.D. and L.Z. initially proposed the idea; Y.L. and Y.D. designed and performed most of the experiments; J.L. performed DFT calculations; Y.L., X.Z. and T.W. contributed to field samplings and data analysis; K.L., K.G., A.B., I.N., X.Z., C.G., and L.Z. provided suggestions on the experiments and paper writing; All authors wrote the manuscript.

Competing interests. The authors declare that they have no conflict of interest.

Acknowledgements. We greatly appreciate Dr. Yang Yang and Prof. Keli Han from Dalian institute of chemical physics for NTAS and some helpful discussions.

Financial support. This work was supported by the National Natural Science Foundation of China (No. 21976030 and No. 21677037), National key research and development program of China (2016YFE0112200 and 2016YFC0202700), the Natural Science Foundation of Shanghai (No. 19ZR1471200 and No. 17ZR1440200).

References

Agustine I, Yulinawati H, Gunawan D, Suswantoro E: Potential impact of particulate matter less than 10 micron (PM_{10}) to ambient air quality of Jakarta and Palembang. Iop C Ser Earth Env, 106 https://doi.org/10.1088/1755-1315/106/1/012057, 2018.

Balachandran U, Eror NG: Raman-Spectra Of Titanium-Dioxide. J. Solid State Chem., 42,276-282, https://doi.org/10.1016/0022-4596(82)90006-8, 1982.

Baltrusaitis J, Schuttlefield J, Zeitler E, Grassian VH: Carbon dioxide adsorption on oxide nanoparticle surfaces. Chem. Eng. J., 170,471-481, https://doi.org/10.1016/j.cej.2010.12.041, 2011.

Bao H, Yu S, Tong DQ: Massive volcanic SO_2 oxidation and sulphate aerosol deposition in Cenozoic North America. Nature, 465,909-912, https://doi.org/10.1038/nature09100, 2010.

Bauer SE, Koch D: Impact of heterogeneous sulfate formation at mineral dust surfaces on aerosol loads and radiative forcing in the Goddard Institute for Space Studies general circulation model. J. Geophys. Res., 110 https://doi.org/10.1029/2005jd005870, 2005.

Beig G, Brasseur GP: Model of tropospheric ion composition: A first attempt. J. Geophys. Res., 105,22671-22684, https://doi.org/10.1029/2000JD900119, 2000.

Bhattacharya A, Amitabha D, Mandal PC: Carbonate radical induced polymerisation of pyrrole: A steady state and flash photolysis study. J. Radioanal Nucl. Ch., 230,91-95, https://doi.org/10.1007/BF02387452, 1998.

Bisby RH, Johnson SA, Parker AW, Tavender SM: Time-resolved resonance Raman spectroscopy of the carbonate radical. J. Chem. Soc. Faraday Trans., 94,2069-2072, https://doi.org/10.1039/A801239C, 1998.

Busset C, Mazellier P, Sarakha M, De Laat J: Photochemical generation of carbonate radicals and their reactivity with phenol. J. Photoch. Photobio. A, 185,127-132, https://doi.org/10.1016/j.jphotochem.2006.04.045, 2007.

Buxton GV, Greenstock CL, Helman WP, Ross AB: Critical Review of rate constants for reactions of hydrated electrons, hydrogen atoms and hydroxyl radicals ($\cdot OH/\cdot O^-$ in aqueous solution. J. Phys. Chem. Ref. Data, 17,513-886, https://doi.org/10.1063/1.555805, 2009.

Cao JJ, Lee SC, Zhang XY, Chow JC, An ZS, Ho KF, et al.: Characterization of airborne carbonate over a site near Asian dust source regions during spring 2002 and its climatic and environmental significance. J. Geophys. Res., 110,1-8, https://doi.org/10.1029/2004JD005244, 2005.

Chameides WL, Davis DD: The Free-Radical chemistry of cloud droplets and its impact upon the composition of rain. J. Geophs Res. Oceans, 87,4863-4877, https://doi.org/10.1029/JC087iC07p04863, 1982.

Chandrasekaran K, Thomas JK: Photochemical reduction of carbonate to formaldehyde on TiO_2 powder. Chem. Phys. Lett., 99,7-10, https://doi.org/10.1016/0009-2614(83)80259-0, 1983.

Chen HH, Nanayakkara CE, Grassian VH: Titanium Dioxide Photocatalysis in Atmospheric Chemistry. Chem Rev, 112,5919-5948, https://doi.org/10.1021/cr3002092, 2012.

Chen Y, Tong SR, Li WR, Liu YP, Tan F, Ge MF, et al.: Photocatalytic Oxidation of SO_2 by TiO_2: Aerosol Formation and the Key Role of Gaseous Reactive Oxygen Species. Environ. Sci. Technol., 55,9784-9793, https://doi.org/10.1021/acs.est.1c01608, 2021.

Cheung K, Daher N, Kam W, Shafer MM, Ning Z, Schauer JJ, et al.: Spatial and temporal variation of chemical composition and mass closure of ambient coarse particulate matter ($PM_{10-2.5}$) in the Los Angeles area. Atmos. Environ., 45,2651-2662, https://doi.org/10.1016/j.atmosenv.2011.02.066, 2011.

Cope VW, Chen S-N, Hoffman MZ: Intermediates in the photochemistry of of carbonato-amine complexes of cobalt(III). carbonate(-) radicals and the aquocarbonato complex. J. Am. Chem. Soc., 95,3116-3121, https://doi.org/10.1021/ja00791a005, 1973

Cwiertny DM, Young MA, Grassian VH: Chemistry and photochemistry of mineral dust aerosol. Annu. Rev. Phys. Chem., 59,27-51, https://doi.org/10.1146/annurev.physchem.59.032607.093630, 2008.

Das TN: Reactivity and role of SO_5.- radical in aqueous medium chain oxidation of sulfite to sulfate and atmospheric sulfuric acid generation. J. Phys. Chem. A, 105,9142-9155, https://doi.org/10.1021/jp011255h, 2001.

Davis AC, Francisco JS: Reactivity trends within alkoxy radical reactions responsible for chain branching. J. Am. Chem. Soc., 133,18208-18219, https://doi.org/10.1021/ja204806b, 2011.

Deng W, Zhao HL, Pan FP, Feng XH, Jung B, Abdel-Wahab A, et al.: Visible-light-driven photocatalytic degradation of organic water pollutants promoted by sulfite addition. Environ. Sci. Technol., 51,13372-13379, https://doi.org/10.1021/acs.est.7b06200, 2017.

Deng Y, Liu Y, Wang T, Cheng H, Feng Y, Yang Y, et al.: Photochemical reaction of CO_2 on atmospheric mineral dusts. Atmos. Environ., 223,117222.1-117222.10, https://doi.org/10.1016/j.atmosenv.2019.117222, 2020.

Dong JL, Xiao HS, Zhao LJ, Zhang YH: Spatially resolved Raman investigation on phase separations of mixed $Na_2SO_4/MgSO_4$ droplets. J. Raman. Spectrosc., 40,338-343, https://doi.org/10.1002/jrs.2132, 2009.

Dotan I, Davidson JA, Streit GE, Albritton DL, Fehsenfeld FC: A study of the reaction $O^{-3}+CO_2 \sim CO^{-3}+O_2$ and its implication on the thermochemistry of CO_3 and O_3 and their negative ions. J. Chem. Phys., 67,2874-2879, https://doi.org/10.1063/1.435155, 1977.

Dupart Y, King SM, Nekat B, Nowak A, Wiedensohler A, Herrmann H, et al.: Mineral dust photochemistry induces nucleation events in the presence of SO_2. Proc. Natl. Acad. Sci. USA, 109,20842-20847, https://doi.org/10.1073/pnas.1212297109, 2012.

El Zein A, Romanias MN, Bedjanian Y: Kinetics and Products of Heterogeneous Reaction of HONO with Fe_2O_3 and Arizona Test Dust. Environ. Sci. Technol., 47,6325-6331, https://doi.org/10.1021/es400794c, 2013.

Fang T, Guo H, Zeng L, Verma V, Nenes A, Weber RJ: Highly Acidic Ambient Particles, Soluble Metals, and Oxidative Potential: A Link between Sulfate and Aerosol Toxicity. Environ. Sci. Technol., 51,2611-2620, https://doi.org/10.1021/acs.est.6b06151, 2017.

Fang X, Liu Y, Kejian, Tao W, Yue D, Yiqing F, et al.: Atmospheric Nitrate Formation through Oxidation by carbonate radical. ACS Earth Space Chem., ASAP https://doi.org/10.1021/acsearthspacechem.1c00169, 2021.

Ferrer-Sueta G, Vitturi D, Batinic-Haberle I, Fridovich I, Goldstein S, Czapski G, et al.: Reactions of manganese porphyrins with peroxynitrite and carbonate radical anion. J. Biol. Chem., 278,27432-27438, https://doi.org/10.1074/jbc.M213302200, 2003.

Ghalei M, Ma J, Schmidhammer U, Vandenborre J, Fattahi M, Mostafavi M: Picosecond pulse radiolysis of highly concentrated carbonate solutions. J. Phys. Chem. B, 120,2434-2439, https://doi.org/10.1021/acs.jpcb.5b12405, 2016.

Goldstein S, Czapski G, Lind J, Merényi G: Carbonate radical ion is the only observable intermediate in the reaction of peroxynitrite with CO_2. Chem. Res. Toxicol., 14,1273-1276, https://doi.org/10.1021/tx0100845, 2001.

Graedel TE, Weschler CJ: Chemistry within Aqueous Atmospheric Aerosols And Raindrops. J. Geophys. Res., 19,505-539, https://doi.org/10.1029/RG019i004p00505, 1981.

Hanisch F, Crowley JN: Ozone decomposition on Saharan dust: an experimental investigation. Atmos. Chem. Phys. Disscuss., 3,119-130, https://doi.org/10.5194/acp-3-119-2003, 2003.

Hayon E, Treinin A, Wilf J: Electronic spectra, photochemistry, and autoxidation mechanism of the sulfite-bisulfite-pyrosulfite systems. SO_2^-, SO_3^-, SO_4^-, and SO_5^- radicals. J. Am. Chem. Soc., 94,47-57, https://doi.org/10.1021/ja00756a009, 1972.

Hossain MD, Huang Y, Yu TH, Goddard Iii WA, Luo Z: Reaction mechanism and kinetics for CO_2 reduction on nickel single atom catalysts from quantum mechanics. Nat. Commun., 11,2256, https://doi.org/10.1038/s41467-020-16119-6, 2020.

Huang HL, Chao W, Lin JJM: Kinetics of a Criegee intermediate that would survive high humidity and may oxidize atmospheric SO_2. Proc. Natl. Acad. Sci. USA, 112,10857-10862, https://doi.org/10.1073/pnas.1513149112, 2015.

Hung HM, Hsu MN, Hoffmann MR: Quantification of SO_2 oxidation on interfacial surfaces of acidic micro-droplets: Implication for ambient sulfate formation. Environ. Sci. Technol., 52,9079-9086, https://doi.org/10.1021/acs.est.8b01391, 2018.

Kerminen VM, Hillamo R, Teinilä K, Pakkanen T, Allegrini I, Sparapani R: Ion balances of size-resolved tropospheric aerosol samples: implications for the acidity and atmospheric processing of aerosols. Atmos. Environ., 35,5255-5265, https://doi.org/10.1016/S1352-2310(01)00345-4, 2001.

Kim H, Zhang Q, Heo J: Influence of Intense secondary aerosol formation and long range transport on aerosol chemistry and properties in the Seoul Metropolitan Area during spring time Results from KORUS-AQ. Atmos. Chem. Phys. Disscuss., https://doi.org/10.5194/acp-2017-947, 2017.

Koelemeijer R, Homan CD, Matthijsen J: Comparison of spatial and temporal variations of aerosol optical thickness and particulate matter over Europe. Atmos. Environ., 40,5304-5315, https://doi.org/10.1016/j.atmosenv.2006.04.044, 2006.

Lehtipalo K, Rondo L, Kontkanen J, Schobesberger S, Jokinen T, Sarnela N, et al.: The effect of acid-base clustering and ions on the growth of atmospheric nano-particles. Nat. Commun., 7,11594, https://doi.org/10.1038/ncomms11594, 2016.

Li BQ, Ma XY, Li QS, Chen WZ, Deng J, Li GX, et al.: Factor affecting the role of radicals contribution at different wavelengths, degradation pathways and toxicity during UV-LED/chlorine process. Chem. Eng. J., 392 https://doi.org/10.1016/j.cej.2020.124552, 2020.

Li KJ, Kong LD, Zhanzakova A, Tong SY, Shen JD, Wang T, et al.: Heterogeneous conversion of SO_2 on nano alpha-Fe2O_3: the effects of morphology, light illumination and relative humidity. Environ. Sci. Nano., 6,1838-1851, https://doi.org/10.1039/c9en00097f, 2019.

Li X, Yu J, Jaroniec M: Hierarchical photocatalysts. Chem. Soc. Rev., 45,2603-2636, https://doi.org/10.1039/c5cs00838g, 2016.

Liao LF, Lien CF, Shieh DL, Chen MT, Lin JL: FTIR study of adsorption and photoassisted oxygen isotopic exchange of carbon monoxide, carbon dioxide, carbonate, and formate on TiO_2. J. Phys. Chem. B, 106,11240-11245, https://doi.org/10.1021/jp0211988, 2002.

Liu Y, He X, Duan X, Fu Y, Dionysiou DD: Photochemical degradation of oxytetracycline: Influence of pH and role of carbonate radical. Chem. Eng. J., 276,113-121, https://doi.org/10.1016/j.cej.2015.04.048, 2015.

Liu Y, Wang T, Fang X, Deng Y, Cheng H, Fu H, et al.: Impact of greenhouse gas CO_2 on the heterogeneous reaction of SO_2 on Alpha-Al_2O_3. Chinese Chem. Lett.,2712-2716, https://doi.org/10.1016/j.cclet.2020.04.037, 2020a.

Liu Y, Wang T, Fang X, Deng Y, Cheng H, Fu H, et al.: Impact of greenhouse gas CO_2 on the heterogeneous reaction of SO_2 on Alpha-Al_2O_3. Chinese Chem. Lett., https://doi.org/10.1016/j.cclet.2020.04.037, 2020b.

Liu ZR, Xie YZ, Hu B, Wen TX, Xin JY, Li XR, et al.: Size-resolved aerosol water-soluble ions during the summer and winter seasons in Beijing: Formation mechanisms of secondary inorganic aerosols. Chemosphere, 183,119-131, https://doi.org/10.1016/j.chemosphere.2017.05.095, 2017.

Long SL, Zeng JR, Li Y, Bao LM, Cao LL, Liu K, et al.: Characteristics of secondary inorganic aerosol and sulfate species in size-fractionated aerosol particles in Shanghai. J. Environ. Sci. China, 26,1040-1051, https://doi.org/10.1016/S1001-0742(13)60521-5, 2014.

McNaughton CS, Clarke AD, Kapustin V, Shinozuka Y, Howell SG, Anderson BE, et al.: Observations of heterogeneous reactions between Asian pollution and mineral dust over the eastern north Pacific during INTEX-B. Atmos. Chem. Phys., 9,8283-8308, https://doi.org/10.5194/acpd-9-8469-2009, 2009.

Merouani S, Hamdaoui O, Saoudi F, Chiha M, Petrier C: Influence of bicarbonate and carbonate ions on sonochemical degradation of Rhodamine B in aqueous phase. J. Hazard Mater., 175,593-599, https://doi.org/10.1016/j.jhazmat.2009.10.046, 2010.

Miller-Schulze JP, Shafer M, Schauer JJ, Heo J, Solomon PA, Lantz J, et al.: Seasonal contribution of mineral dust and other major components to particulate matter at two remote sites in Central Asia. Atmos. Environ., 119,11-20, https://doi.org/10.1016/j.atmosenv.2015.07.011, 2015.

Mogili PK, Kleiber PD, Young MA, Grassian VH: Heterogeneous uptake of ozone on reactive components of mineral dust aerosol: an environmental aerosol reaction chamber study. J. Phys. Chem. A, 110,13799-807, https://doi.org/10.1021/jp063620g, 2006.

Möller F: On the influence of changes in the CO_2 concentration in air on the radiation balance of the Earth's surface and on the climate. Journal of Geophysical Research, 68,3877-3886, https://doi.org/10.1029/JZ068i013p03877, 1964.

Nanayakkara CE, Larish WA, Grassian VH: Titanium dioxide nanoparticle surface reactivity with atmospheric gases, CO_2, SO_2, and NO_2: roles of surface hydroxyl groups and adsorbed water in the formation and stability of adsorbed products. J. Phys. Chem. C, 118,23011-23021, https://doi.org/10.1021/jp504402z, 2014.

Neta P, Huie RE: Free-radical chemistry of sulfite. Environ. Health Persp., 64,209-217, https://doi.org/10.1289/ehp.8564209, 1985.

None: In-Situ Characterization of Heterogeneous Catalysts. Focus on Catal., 2013,8, https://doi.org/10.1016/S1351-4180(13)70477-X, 2013.

Peters SJ, Ewing GE: Water on Salt: An Infrared Study of Adsorbed H_2O on NaCl (100) under Ambient Conditions. J. Phys. Chem. B, 101,10880-10886, https://doi.org/https://doi.org/10.1021/jp972810b, 1997.

Platt U, Lebras G, Poulet G, Burrows JP, Moortgat G: Peroxy radicals from night-time reaction of NO_3 with organic compounds. Nature, 348,147-149, https://doi.org/10.1038/348147a0, 1990.

Prinn RG, Huang J, Weiss RF, Cunnold DM, Fraser PJ, Simmonds PG, et al.: Evidence for substantial variations of atmospheric hydroxyl radicals in the past two decades. Science, 292,1882-1888, https://doi.org/10.1126/science.1058673, 2001.

Salama SB, Natarajan C, Nogami G, Kennedy JH: The role of reducing agent in oxidation reactions of water on illuminated TiO_2 electrodes. J. Electrochem. Soc., 142,806-810, https://doi.org/10.1149/1.2048539, 1995.

Shafirovich V, Dourandin A, Huang W, Geacintov NE: The carbonate radical is a site-selective oxidizing agent of guanine in double-stranded oligonucleotides. J. Biol. Chem., 276,24621-24626, https://doi.org/10.1074/jbc.M101131200, 2001.

Shang J, Li J, Zhu T: Heterogeneous reaction of SO_2 on TiO_2 particles. Sci. China Chem., 53,2637-2643, https://doi.org/10.1007/s11426-010-4160-3, 2010.

Song X, Li J, Shao L, Zheng Q, Zhang D: Inorganic ion chemistry of local particulate matter in a populated city of North China at light, medium, and severe pollution levels. Sci.Total. Envrion., 650,566-574, https://doi.org/10.1016/j.scitotenv.2018.09.033, 2018.

Stenman D, Carlsson M, Jonsson M, Reitberger T: Reactivity of the carbonate radical anion towards carbohydrate and lignin model compounds. J. Wood Chem. Technol., 23,47-69, https://doi.org/10.1081/Wct-120018615, 2003.

Stone R: Air pollution. Counting the cost of London's killer smog. Science, 298,2106-2107, https://doi.org/10.2307/3833025, 2002.

Su H, Cheng Y, Zheng G, Wei C, Mu Q, Zheng B, et al.: Reactive nitrogen chemistry in aerosol water as a source of sulfate during haze events in China. Sci. Adv., 2,e1601530, https://doi.org/10.1126/sciadv.1601530, 2016.

Su WG, Zhang J, Feng ZC, Chen T, Ying PL, Li C: Surface phases of TiO_2 nanoparticles studied by UV Raman spectroscopy and FT-IR spectroscopy. J. Phys. Chem. C, 112,7710-7716, https://doi.org/10.1021/jp7118422, 2008.

Sullivan RC, Guazzotti SA, Sodeman DA, Prather KA: Direct observations of the atmospheric processing of Asian mineral dust. Atmos. Chem. Phys., 7,1213-1236, https://doi.org/10.5194/acp-7-1213-2007, 2007.

Sulzberger B, Canonica S, Egli T, Giger W, Klausen J, Gunten Uv: Oxidative transformations of contaminants in natural and in technical systems. Chimia, 51,900-907, https://doi.org/10.1051/epjconf/20101105003, 1997.

Sun P, Tyree C, Huang CH: Inactivation of Escherichia coli, Bacteriophage MS2, and Bacillus Spores under UV/H_2O_2 and UV/Peroxydisulfate Advanced Disinfection Conditions. Environ. Sci. Technol., 50,4448-4458, https://doi.org/10.1021/acs.est.5b06097, 2016.

Thompson AM: The oxidizing capacity of the earth's atmosphere: probable past and future changes. Science, 256,1157-1165, https://doi.org/10.1126/science.256.5060.1157, 1992.

Wang XK, Gemayel R, Hayeck N, Perrier S, Charbonnel N, Xu CH, et al.: Atmospheric Photosensitization: A New Pathway for Sulfate Formation. Environ. Sci. Technol., 54,3114-3120, https://doi.org/10.1021/acs.est.9b06347, 2020.

Wang Y, Wan Q, Meng W, Liao F: Long-term impacts of aerosols on precipitation and lightning over the Pearl River Delta megacity area in China. Atmos. Chem. Phys., 11,12421-12436, https://doi.org/10.5194/acp-11-12421-2011, 2011.

Wei J, Yu H, Wang Y, Verma V: Complexation of Iron and Copper in Ambient Particulate Matter and Its Effect on the Oxidative Potential Measured in a Surrogate Lung Fluid. Environ. Sci. Technol., 53,1661-1671, https://doi.org/10.1021/acs.est.8b05731, 2019.

Witkowska A, Lewandowska AU, Saniewska D, Falkowska LM: Effect of agriculture and vegetation on carbonaceous aerosol concentrations (PM2.5 and PM10) in Puszcza Borecka National Nature Reserve (Poland). Air Qual Atmos Hlth, 9,761-773, https://doi.org/10.1007/s11869-015-0378-8, 2016.

Wu C, Zhang S, Wang G, Lv S, Li D, Liu L, et al.: Efficient Heterogeneous Formation of Ammonium Nitrate on the Saline Mineral Particle Surface in the Atmosphere of East Asia during Dust Storm Periods. Environ. Sci. Technol., 54,15622-15630, https://doi.org/10.1021/acs.est.0c04544, 2020.

Wu D, Fan Z, Ge X, Meng Y, Xia J, Liu G, et al.: Chemical and Light Extinction Characteristics of Atmospheric Aerosols in Suburban Nanjing, China. Atmosphere, 8,149, https://doi.org/10.3390/atmos8080149, 2017.

Xia DM, Zhang XR, Chen JW, Tong SR, Xie HB, Wang ZY, et al.: Heterogeneous Formation of HONO Catalyzed by CO_2. Environ. Sci. Technol., 55,12215-12222, https://doi.org/10.1021/acs.est.1c02706, 2021.

Xiong XQ, Zhang X, Xu YM: Incorporative effect of Pt and Na_2CO_3 on TiO_2-photocatalyzed degradation of phenol in water. J. Phys. Chem. C, 120,25689-25696, https://doi.org/10.1021/acs.jpcc.6b07951, 2016.

Yan JF, Peng JL, Lai LD, Ji FZ, Zhang YH, Lai B, et al.: Activation $CuFe_2O_4$ by Hydroxylamine for Oxidation of Antibiotic Sulfamethoxazole. Environ. Sci. Technol., 52,14302-14310, https://doi.org/10.1021/acs.est.8b03340, 2018.

Yan SW, Liu YJ, Lian LS, Li R, Ma JZ, Zhou HX, et al.: Photochemical formation of carbonate radical and its reaction with dissolved organic matters. Water Res., 161,288-296, https://doi.org/10.1016/j.watres.2019.06.002, 2019.

Yann Batonneau, Sophie Sobanska, Jacky Laureyns, Bremard C: Confocal microprobe Raman imaging of urban tropospheric aerosol particles. Environ. Sci. Technol., 40,1300-1306, https://doi.org/10.1021/es051294x, 2008.

Yermakov AN, Purmal AP: Iron-catalyzed oxidation of sulfite: From established results to a new understanding. Prog. React. Kinet. Mec., 28,189-255, https://doi.org/10.3184/007967403103165503, 2003.

Yu T, Zhao D, Song X, Zhu T: NO_2-initiated multiphase oxidation of SO_2 by O_2 on $CaCO_3$ particles. Atmos. Chem. Phys., 18,6679-6689, https://doi.org/10.5194/acp-18-6679-2018, 2018.

Zhang GS, He XX, Nadagouda MN, O'Shea KE, Dionysiou DD: The effect of basic pH and carbonate ion on the mechanism of photocatalytic destruction of cylindrospermopsin. Water Res., 73,353-361, https://doi.org/10.1016/j.watres.2015.01.011, 2015a.

Zhang R, Wang G, Song G, Zamora ML, Qi Y, Yun L, et al.: Formation of urban fine particulate matter. Chemical Reviews, 115,3803-3855, https://doi.org/10.1021/acs.chemrev.5b00067, 2015b.

Zheng B, Zhang Q, Zhang Y, He KB, Wang K, Zheng GJ, et al.: Heterogeneous chemistry: a mechanism missing in current models to explain secondary inorganic aerosol formation during the January 2013 haze episode in north China. Atmos. Chem. Phys., 15,2031-2049, https://doi.org/10.5194/acp-15-2031-2015, 2015.